

Recombinant PAI-1 inhibits angiogenesis and reduces size of LNCaP prostate cancer xenografts in SCID mice

RAFAL SWIERCZ^{1,3}, RICK W. KECK^{1,2}, EWA SKRZYPCZAK-JANKUN^{1,4},
STEVEN H. SELMAN¹⁻³, and JERZY JANKUN¹⁻⁴.

¹Urology Research Center, ²Department of Urology, ³Physiology and Molecular Medicine, Medical College of Ohio, Toledo, OH 43614-5807; ⁴Department of Chemistry, The University of Toledo Toledo, OH 43606-3390, USA.

Received February 14, 2001; Accepted March 1, 2001

Abstract. To understand the fundamental determinants of urokinase plasminogen activator (uPA) driven angiogenesis in cancer we studied how inhibition of uPA activity could reduce neovascularization and consequently reduce tumor size in experimental animals. Proteolytic enzymes are required to mediate tumor cell invasion to adjacent tissues and initiate the metastatic process. Many different human cancers commonly overexpresses the urokinase plasminogen activator system, one of the proteolytic enzyme systems. Reduction of urokinase (uPA) activity in cancer cells is evidently associated with diminished invasion and metastasis. However, it has been shown recently that inhibitors of uPA could reduce tumor size also. The mechanism of action leading to decline in tumor growth rate is not clear. Proteolysis is responsible for degradation of proteins, for invasion or metastasis, but not for the proliferate properties of the cancer cells. It is difficult to envision that diminishing the size of tumor is due to simply blocking of uPA activity of cancer cells. Instead, inhibitors of uPA may be interacting with the elements of the extracellular matrix, such the neovascular bed surrounding tumors that has been reported to contain high amounts of uPA and its receptor. Overall these data strongly suggest that inhibitors of urokinase limit cancer growth by inhibiting the angiogenesis. However, it is possible also that uPA inhibitors could act on cancer cells directly or prevent angiogenesis by alternative mechanisms that are not related to uPA inhibition. Therefore, we examined if plasminogen activator inhibitor (PAI-1) could limit angiogenesis. If it does, it will provide definitive evidence of uPA/PAI-1 involvement in reduction of cancer growth. Indeed, our study demonstrates that exogenously applied 14-1b PAI-1 is powerful inhibitor of angiogenesis in

three different *in vitro* models and is powerful anti-cancer agent in SCID mice model inoculated with human LNCaP prostate cancer cells.

Introduction

Metastasis is the cause of most cancer-related death. The proteolytic degradation of the extracellular matrix is recognized as a mechanism that plays an important role in the metastatic process. Proteolytic enzymes are required to mediate tumor cell invasion into adjacent tissues and initiate the metastatic process. Urokinase plasminogen activator (uPA) is commonly overexpressed by many different human cancers (1).

The uPA system contains the following elements: (i) Plasminogen – a non-active enzyme that is cleaved to form the active plasmin. Plasmin is a strong proteolytic enzyme able to digest proteins of connective tissue and basement membranes. Plasmin can activate other latent proteolytic enzymes, thus broadening the spectrum of proteins attacked. Pro-collagenase is activated to collagenase in this way. Plasmin is a key enzyme in tissue remodeling, tumor invasion and development of distant metastasis. (ii) Activators - uPA and tissue plasminogen activator (tPA). Both are weak proteolytic enzymes that activate plasminogen to plasmin by proteolytic cleavage. uPA is involved in pericellular proteolysis during cell migration, wound healing, and tissue remodeling under a variety of physiological and pathological conditions. tPA mainly mediates intravascular thrombolysis (1, 5, 20). (iii) Inhibitors of plasminogen activators. There are four proteins known for their inhibitory activity toward uPA: PAI-1, PAI-2, PAI-3 and a protein called nexin. All are regulatory proteins mediating proteolysis at the activation level. Most relevant in the metastatic process is PAI-1, which exists in three different forms: nonactive-latent, cleaved, and the active form. (iv) uPAR, a uPA receptor is a glycoprotein that binds uPA to the cell surface. Surface bound uPA retains its ability to activate plasminogen. High numbers of uPA receptors on the surface of cancer cells, if occupied by uPA, create elevated proteolytic activity in the proximity of cancer cells (13).

An increased amount or activity of uPA or uPAR per cell has been found in human cancer cells lines with metastatic behavior (2). Animals injected with cancer cells expressing higher amounts of uPA and/or uPAR develop metastatic lesions earlier and more frequently than animals injected with the same cell expressing lower amounts of uPA/uPAR (3). Additionally, it has

Correspondence to: Dr. Jerzy Jankun, Urology Research Center, Medical College of Ohio, Toledo, OH 43614-5807, USA

e-mail: jerzy@golemxiv.dh.mco.edu

Key Words: urokinase, plasminogen activator inhibitor-1, prostate, cancer, angiogenesis.

been reported that uPA activity is increased in metastatic tumors compared with primary tumors in experimental animals (4). The ability of human carcinoma cells to metastasize to chick embryo was dramatically reduced when cells were treated with the antibody against the active site of uPA (5). Prostate cancer cells transfected with a plasmid overexpressing of uPA in prostate cancer cells showed a marked increase in metastasis, in comparison with the parental cell phenotype in the rat model. Cells from the same phenotype underexpressing uPA displayed drastically decreased metastasis (3). The other plasminogen activator tPA, is rarely overexpressed in malignant tumors and does not seem to be relevant in the metastatic process (11).

Reduction of uPA activity in cancer cells is clearly associated with diminished invasion and metastasis; however, it has also been recently shown that inhibitors of uPA can reduce tumor size. Billstrom *et al.* (6) showed that p-aminobenzamidine, a competitive inhibitor of uPA, caused a dose-dependent inhibition of uPA activity and decreased tumor-growth in SCID mice inoculated with DU-145 human prostate cancer cells when compared with non-treated animals. Amiloride, another uPA inhibitor, reduces tumor growth and decreases the proliferation of tumor cells in hepatomas and intestinal carcinomas (7-9).

Traditional thought holds that reduction of proteolytic activity will reduce invasion and metastasis of cancer cells (5,11,12). In this way uPA inhibitors could have an important yet somewhat limited application in therapy because, at the time of diagnosis metastatic micro foci are already formed. Far more interesting is the ability of uPA inhibitors to reduce tumor growth. The mechanism of action leading to a decline in tumor growth rate is not clear. Proteolysis is responsible for degradation of proteins, for invasion or metastasis, but not for the proliferate properties of cancer cells. It is difficult to envision that diminishing tumor is due to blocking the uPA activity of cancer cells. It is more likely that inhibitors of uPA may be interacting with elements of the extracellular matrix, that express uPA. For example, the neovascular bed surrounding tumors has been reported to contain high amounts of uPA and its receptor (23). Binding of proteolytically inactive ligands to uPA receptor reduces the amount of uPA on the surface of capillary endothelial cells and reduces tumor growth (18). Indeed, our studies have shown that uPA inhibitors decrease angiogenesis in the chicken embryo model (19). Rosenberg has shown that binding of proteolytically inactive uPAR ligands, prevents cell surface plasminogen activation and consequently prevents angiogenesis in the mouse model (21). He emphasized that the uPAR focuses uPA and initiates proteolytic activity on the vascular capillary cell surface, which is required for angiogenesis. Ignjatovic observed inhibition of angiogenesis in the rabbit cornea, while treating animals with amiloride, a competitive inhibitor of uPA (22).

Overall, these data strongly suggest that inhibitors of urokinase limit cancer growth by inhibiting angiogenesis. However, it is possible that uPA inhibitors can act on cancer cells directly or prevent angiogenesis by an alternative mechanism not related to uPA inhibition. For example, amiloride has been postulated to be an anti-cancer agent based on the cellular acidification (17). Therefore, we

examined if PAI-1 could limit angiogenesis and consequently the growth of cancers in experimental animals. If PAI-1 limits angiogenesis, it would provide crucial evidence of the uPA/PAI-1 pathway involvement in the reduction of cancer growth by hindering angiogenesis.

The most difficult aspect of testing this hypothesis is the rapid conversion of wild type PAI-1 from its active form to its latent form with half-life of approximately 2h. Fortunately, quadruple mutant of PAI-1 with half-life of 156h has been produced and we have been using this protein in our studies (25).

Materials and Methods

Obtaining the starting structure. All molecular modeling and structure visualization were done on a SGI workstation using the *InsightII* program package from Molecular Structure Inc., CA (32). Atomic coordinates of latent and active PAI-1 were retrieved from the Protein Data Bank (latent, entry 1C5G (14, 15) and active, entry 1B3K (16)). Hydrogen atoms were added and appropriate charges assigned throughout the PAI-1 molecules assuming a physiological pH 7.4.

Construction of expression plasmids. The human PAI-1 14-1b mutant cDNA (from D. Ginsburg, University of Michigan, Ann Arbor) was excised from pQE30-PAI vector as a *NdeI/NsiI* fragment and separated from pQE30 vector by DNA agarose gel electrophoresis. This fragment was then ligated using T4 DNA ligase into *NdeI/PstI*-cut pTYB-12 vector to create pTYB12-PAI1 plasmid, which was then transformed into *E. coli* strain ER2567 by rubidium chloride precipitation. Transformed cells were seeded on agar containing ampicillin (100µg/ml) and grown overnight at 37 °C. Single colonies were transferred to test tubes containing 6 ml of LB-broth and ampicillin and grown overnight. pTYB12-PAI1 plasmid DNA was isolated by alkaline lysis. Purified plasmid DNA was subjected to restriction analysis to determine that 14-1b PAI-1 cDNA was incorporated into pTYB12 vector by digestion with *NdeI* and *BspI* restriction enzymes. Finally, pTYB12-PAI-1 plasmid DNA was then transformed by rubidium chloride precipitation into ER2566 *E. coli* strain, which has the T7 polymerase gene incorporated into its genome.

DNA sequencing. The DNA sequence of the 14-1b human PAI-1 mutant was determined using the Sanger (Dideoxy) method (35). For the sequencing we used two forward primers:

5'-CCCGAAAAGTGCCACCTG-3';
5'-AGTGGACTTTTCAGAGGTGGAG-3'

and two reverse primers:

5'-GTTCTGAGGTCATTACTGG-3';
5'-GTCGGTCATTCCGACGTTCT-3'.

In this method, pTYB12-PAI1 plasmid DNA solution was added with primer solution, deoxynucleotide mix, thermosequense DNA polymerase solution and one of four ³³P – radiolabelled dideoxynucleotide solutions. The reaction was cycled for 60 minutes as follows: 95°C – 30 s; 55°C – 30 s; 72°C – 60 s. Reactions were terminated by addition of Stop solution (95% formamide, 20 mM EDTA, 0.05% bromophenol blue, 0.05%

xylene cyanol FF). Samples were heated at 70°C for 5 minutes before electrophoretic size fractionation on polyacrylamide gels in GATC order, followed by autoradiography. The DNA sequence of 14-1b PAI-1 was read manually and determined sequences were aligned using of CloneMap software (Version 2.11; CGC Scientifics, Inc; CA) to determine the entire DNA sequence of 14-1b PAI-1.

Purification of PAI-1 14-1b. One liter of fresh LB broth containing ampicillin was inoculated and incubated at 37 °C, until the OD₆₀₀ of the cell culture reached ~0.6. The expression of the 14-1b PAI-1 was stimulated by the addition of IPTG to a final concentration of 0.5 mM and cells were incubated overnight at 20 °C. Cells were spun down, and the cell pellet was washed with 50 ml ice cold Cell Lysis Buffer (20 mM Na-HEPES, 500 mM NaCl, 1mM EDTA, 20 μM PMSF, 5 Mm MgCl₂, 10 μg/ml protease-free Dnase; pH = 8.00). After washing, cells were resuspended in 30 ml of Cell Lysis Buffer and broken down with French press. The cellular debris was removed by centrifugation and clear crude cell extract was transferred to a new tube and stored in the freezer at -20 °C.

PAI-1 14-1b was isolated by affinity chromatography on intein binding column. 30 ml of chitin bead resin was equilibrated with 10 bed volumes of Column Buffer (20 mM HEPES, 500 mM NaCl, 1 mM EDTA; pH = 8.00). Crude cell extract was applied on the column with 0.5 ml/min flow rate. The column was washed with 20 bed volumes of column buffer at 1.0 ml/min flow rate to remove unbound proteins then flushed with 3 bed volumes of Cleavage Buffer (20 mM HEPES, 500 mM NaCl, 1 mM EDTA, 50 mM DTT; pH = 8.00) at 2.0 ml/min and incubated for 40 h at 4 °C to stimulate on-column cleavage. The released from intein purification tag PAI-1 14-1b mutant was eluted from the column with Column Buffer. The eluted PAI-1 was dialyzed overnight against PBS Buffer (120 mM NaCl, 2.7 mM KCl, 10 mM Na₃PO₄; pH 7.40) and concentrated. The yield was approximately 15-20 mg/l of cell culture.

Western blot analysis. Purified 14-1b PAI-1 in Loading Buffer (0.5 M Tris-HCl, pH = 6.80; 10% Glycerol; 10% SDS; 0.1% bromophenol blue; 2.7 mM β-mercaptoethanol) and subjected to SDS-PAGE (10% gel). Next, the gel was equilibrated in Transfer Buffer (20% methanol, 193 mM glycine, 25 mM Tris-HCl) for 5 minutes after the run and proteins from the polyacrylamide gel were transferred to a nitrocellulose membrane (0.45 μm) at 100 V for 2 hours. The nitrocellulose membrane was then washed in Blotting Buffer (PBS pH = 7.40; 0.05% Tween-20), blocked in 5% non-fat milk in Blotting Buffer for 1 hour at room temperature, and washed. The membrane was then treated with primary goat anti-human PAI-1 antibody (5 μg/ml in Blotting Buffer containing 1 % BSA) for 1 hour at room temperature and washed. The membrane was then treated with secondary horseradish peroxidase (HRP) conjugated anti-goat antibody (1:2000 dilution, in Blotting Buffer containing 1 % BSA) for 1 hour at room temperature and washed. Finally, the membrane was incubated in HRP substrate solution (metal enhanced 3,3'-diamino benzidine

tetrahydrochloride, 1:10 dilution) for 15 minutes at room temperature. After stopping the reaction by rinsing with deionized water, the membrane was allowed to air dry.

u-PA/PAI-1 complex formation assay. In this assay, 20 μl of u-PA solution (2.0 mg/ml stock solution in Coupling Buffer; 50 mM Na₃PO₄; 150 mM NaCl; 1 mM EDTA; pH = 7.00) was mixed with 40, 50, and 60 μl of PAI-1 solution (2 mg/ml stock solution in Coupling Buffer) and incubated for 30 min at room temperature. Samples were then mixed with a Loading Buffer, and subjected to SDS-PAGE under non-reducing conditions. After the run, polyacrylamide gel was stained in staining solution for 2 hours at room temperature followed by overnight destaining.

Cell line and cell culture conditions. The human prostate cancer cell line LNCaP was purchased from American Type Culture Collection, Rockville, MA. This cell line is negative for uPA (31). The cells were propagated in RPMI-1640 medium (Sigma Chemical Co., St. Louis, MO), and supplemented with 10% fetal bovine serum (Hyclone Laboratories, Logan, UT), penicillin and streptomycin.

The human vascular endothelial cell line HUVEC was purchased from Clonetics, Walkersville, MD. HUVEC cells were grown to 80-90% confluence in EGM-2 growth medium. The cells were then trypsinized and seeded onto 0.5% agarose coated culture dishes. This procedure resulted in cell aggregate formation after 24 h of incubation at +37 °C. The HUVEC aggregates were descended for 30 min at room temperature. The old-medium supernatant was decanted and HUVEC aggregates were suspended in 5 ml of fresh EGM-2 growth medium.

Sprout formation assay. Three-dimensional fibrin gels were prepared by mixing the following in 12-well culture plates: 960 μl of human fibrinogen (Type III, 60 % of protein clotable; 2.50 mg/ml concentration in RPMI-1640 medium), 40 μl of HUVEC aggregate suspension, and 12.5 μl of human thrombin (25 IU/ml concentration in RPMI-1640 medium). The mixture was mixed and allowed to gel for about 4 minutes at +37 °C before adding EGM-2 growth medium over the gel. The HUVEC aggregates were suspended in fibrin gel containing benzamidine (31 μM), B428 (40 nM) and 14-1b PAI-1; 1 ml of EGM-2 growth medium was added over the fibrin gel. The PAI-1 in the fibrin gel was adjusted to a final concentration of 0.50, 0.75, 1.00, 2.00, 3.00; 4.00, and 5.00 μM. The 1B-14 PAI-1 mutant solution used in this study was dialyzed against PBS Buffer (pH = 7.40) overnight at +4 °C. After 3 days of cell incubation, cultures were fixed in situ for 24 h with 2 ml of 10 % formalin solution and photographed under a phase-contrast microscope.

Chicken chorioallantoic membrane (CAM) assay. One-day-old fertilized eggs (purchased from Herzfeld Poultry Farms, Waterville, OH) were incubated for three days in a water-jacketed incubator (38°C, 85% humidity). Next, the eggs were cracked and the chick embryos with intact yolks were placed in plastic Petri dishes containing 10 ml of RPMI-1640 medium. After 3 days of incubation (38°C, 85% humidity, 3% of CO₂), the dialyzing bag (MWCO = 500,000) containing PAI-1 or methylcellulose discs with small molecular inhibitors were placed on the CAMs of the individual embryos. After 48h of incubation, CAM of individual embryo was analyzed for formation of avascular zones and photographed. The angiostatic effect was determined as a percentage of the area of blood vessels under the dialyzing bag or

methylcellulose disks (3-5 eggs for each concentration) in relation to the non-treated areas.

Image processing and analysis. Photographs of the area below the dialysis bag and two non-treated areas were scanned. Color images were converted into black/white images, contrast was enhanced, and images were saved as 16-bitmap files using Paint Software (Microsoft Corporation, Redmond, VA). Next, black/white images were converted into false color (rainbow striped) images using Transform2 Software (Fortner, Sterling, VA). Finally, the area of the blood vessels was calculated using T3D Software (Fortner, Sterling, VA).

LNCaP xenografts in SCID mice and treatment. SCID/BALB-c mice were purchased from the NCI, Fredrick, ME. Forty-two mice (males) were subcutaneously inoculated in the left rear flank with 1.0×10^6 of LNCaP cells in Matrigel®. After 32 days when the tumors were approximately 0.2 cm^3 in size, animals were divided into 6 groups. Control-1 group (n = 7) composed of SCID-mice inoculated with LNCaP tumor cells. Control-2 group (n = 7) composed of SCID-mice inoculated with LNCaP cells and receiving saline solution delivered via subcutaneously implanted ALZET® osmotic pump. There were 4 treatment groups (n = 7, each) composed of SCID-mice inoculated with LNCaP tumor cells and receiving 14-1b human PAI-1 (10, 20, 30, 40 nM). The PAI-1 solution was delivered via an ALZET® osmotic pump.

A 200 μL (model #2004) osmotic pump was used and the 14-1b human PAI-1 and saline solutions were delivered at a flow rate of 0.25 $\mu\text{L}/\text{h}$. Tumor size in each group was measured every 3 days over the 28-day course of the experiment and the volume was calculated using the following formula:

$$V = 4/3 \pi R_1^2 R_2$$

where: V = volume [cm^3]; R_1 = radius; R_2 = radius; and $R_1 > R_2$

Statistical analysis. The statistical analysis was performed using one way ANOVA on Ranks test followed by the Kruskal-Wallis on Ranks test. To isolate the groups that differ from the control group a Dunn's method of multiple comparison was used. All statistical calculations were performed using SigmaStat Software (Jandel Scientific Corp., San Rafael, CA), and significance was established at the level of $P < 0.05$.

Results and discussion

Comparison of molecular structures of latent and active 14-1b PAI-1s. The structure of active PAI-1 differs significantly from its inactive form. In the latent the form reactive loop is buried in the PAI-1 molecule between strands A3 and A5, as A4 strand of the β sheet, and it is not accessible for binding to uPA. However, in the active form, when A4 part slides out, A3 and A5 strands are not

separated by any gap, but come close together and maintain the uniform β sheet. In 14-1b mutant the A3 and A5 strands are stabilized by the new hydrogen bonds of 173 H and 260 G or by sterically more favorable conformations of mutated amino acids of: 173 N \rightarrow H, 177 K \rightarrow T, 342 Q \rightarrow L (15, 16). These mutations might have an effect on other biochemical and biological functions of PAI-1 such as LRP, heparin, α_1 -antitrypsin and vitronectin binding. Therefore, we have analyzed the 3D architecture of superimposed structures of both forms. As expected superposition yield rms deviation of 7.4 \AA when averaging is done over C α atoms. However, despite significant differences in the A3 and A5 strands and the position of active loop, both molecules contain structurally conserved regions of extremely close geometry. Binding sites of LRP, heparin, α_1 -antitrypsin and vitronectin are on the opposite site of A3, A5 strands and contain amino acids 50-130 that are in these conserved regions (16). Superposition of this part of both molecules produces almost identical C α folding with rms of 1.6 \AA (14, 15, 33, and 34). These facts strongly suggest that active 14-1b PAI-1 might be expected to retain biochemical and biological properties of its wild active PAI-1 counterpart such as the ability to bind LRP or vitronectin. Indeed, recently published paper reports vitronectin-binding capability of 14-1b PAI-1 similar to wild form of PAI-1 (27).

Expression and purification of 14-1b PAI-1. The PAI-1 gene was inserted into the plasmid as described in the M&M section. To verify the presence of mutations the entire gene was sequenced. As expected the analysis of the DNA sequence of 1B-14 mutant of the human PAI-1 revealed four mutation sites; (1) 451 AAC \rightarrow CAC, (2) 464 AAA \rightarrow CTG, (3) 958 CAG \rightarrow CTG, (4) 1063 ATG \rightarrow ATA as shown in Figure 1. These correspond to mutations of amino acids at positions, 173 N \rightarrow H, 177 K \rightarrow T, 342 Q \rightarrow L, and 377 M \rightarrow I and these mutations are consistent with published data (25).

PAI-1 purified on column in single step purification process was analyzed by SDS-PAGE. Coomassie-brilliant blue staining of the eluted fractions from the chitin beads column showed that fractions 3 – 5 revealed a single band of 43 kDa molecular weight (as shown in Figure 2 a) which represents the molecular weight of recombinant PAI-1. It was estimated to be at least 96 – 98% pure preparation, and 14-1b PAI-1 was later identified by Western blot analysis using polyclonal goat anti-PAI-1 antibody as shown in Figure 2 b. The immunostaining of nitrocellulose attached crude protein extract revealed single band of 90 kDa, which represents the fusion protein of intein/14-1b PAI-1, while fractions eluted from the column showed only a band of 43 kDa molecular weight.

The activity of purified 14-1b PAI-1 was confirmed by u-PA/PAI-1 complex formation assay. After purification PAI-1 was incubated with LMW u-PA, resulting in the formation of a SDS-stable LMWu-PA/PAI-1 complex seen as 77 kDa line when run on a 10% SDS PAGE (data not shown).

PAI-1 14-b 1 inhibits of sprout formation of human endothelial cells. In this study we have used two types of human endothelial cells, HMVEC (adult origin) and HUVEC (embryonic origin). As there were no significant differences in anti-angiogenic activity of uPA inhibitors between HMVEC and HUVEC, only the results with HUVEC will be discussed.

¹ ATGGTGCACC ATCCCCATC CTACGTGGCC CACCTGGCCT
⁴¹ CAGACTTCGG GGTGAGGGTG TTTCAGCAGG TGGCGCAGGC
⁸¹ CTCCAAGGAC CGCAACGTGG TTTTCTCACC CTATGGGGTG
¹²¹ GCCTCGGTGT TGGCCATGCT CCAGCTGACA ACAGGAGGAG
¹⁶¹ AAACCCAGCA GCAGATTCAA GCAGCTATGG GATTCAAGAT
²⁰¹ TGATGACAAG GGCATGGCCC CCGCCCTCCG GCATCTGTAC
²⁴¹ AAGGAGCTCA TGGGGCCATG GAACAAGGAT GAGATCAGCA
²⁸¹ CCACAGACGC GATCTTCGTC CAGCGGGATC TGAAGCTGGT
³²¹ CCAGGGCTTC ATGCCCCACT TCTTCAGGCT GTTCCGGAGC
³⁶¹ ACGGTCAAGC AAGTGGACTT TTCAGAGGTG GAGAGAGCCA
⁴⁰¹ GATTTCATCAT CAATGACTGG GTGAAGACAC ACACAAAAGG
⁴⁴¹ TATGATCAGC **CAC**TTGCTTG GGA**CAG**GAGC CGTGGACCAG
⁴⁸¹ CTGACACGGC TGGTGTGGT GAATGCCCTC TACTTCAACG
⁵²¹ GCCAGTGGAA GACTCCCTTC CCCGACTCCA GCACCCACCG
⁵⁶¹ CCGCCTCTTC CACAAATCAG ACGGCAGCAC TGTCTCTGTG
⁶⁰¹ CCCATGATGG CTCAGACCAA CAAGTTCAAC TATACTGAGT
⁶⁴¹ TCACCACGCC CGATGGCCAT TACTACGACA TCCTGGAAct
⁶⁸¹ GCCCTACCAC GGGGACACCC TCAGCATGTT CATTGCTGCC
⁷²¹ CCTTATGAAA AAGAGGTGCC TCTCTCTGCC CTCACCAACA
⁷⁶¹ TTCTGAGTGC CCAGCTCATC AGCCACTGGA AAGGCAACAT
⁸⁰¹ GACCAGGCTG CCCCGCCTCC TGGTTCTGCC CAAGTTCTCC
⁸⁴¹ CTGGAGACTG AAGTCGACCT CAGGAAGCCC CTAGAGAACC
⁸⁸¹ TGGGAATGAC CGACATGTTT AGACAGTTTC AGGCTGACTT
⁹²¹ CACGAGTCTT TCAGACCAAG AGCCTCTCCA CGTCGCG**CTG**
⁹⁶¹ GCGCTGCAGA AAGTGAAGAT CGAGGTGAAC GAGAGTGGCA
¹⁰⁰¹ CGGTGGCCTC CTCATCCACA GCTGTCATAG TCTCAGCCCG
¹⁰⁴¹ CATGGCCCCC GAGGAGATCA **ATA**GACAG ACCCTTCCTC
¹⁰⁸¹ TTTGTGGTCC GGCACAACCC CACAGGAACA GTCCTTTTCA
¹¹²¹ TGGGCCAAGT GATGGAACCC TGA

Figure 1. The DNA sequence of recombinant 14-1b human PAI-1. Letters in bold and underlined denote codons of mutated amino acids.

Our results showed that in the absence of the 14-1b PAI-1, the endothelial cell aggregates formed long sprouts, however when 14-1b PAI-1 was added to the fibrin gel there was a significant inhibition of the sprouts length in a dose dependent manner as it is shown in Figure 3. 14-1b PAI tested at concentrations of 1.0; 2.0; 3.0; 4.0; and 5.0 μ M produced statistically significant reduction in length of the developing sprouts. As positive controls we used B-428 and benzamidine which in our previous study (19) showed that these synthetic inhibitors of u-PA are angiostatic agents. As expected these two inhibitors decrease length of sprouts formed by HMVEC and HUVEC aggregates (data not shown).

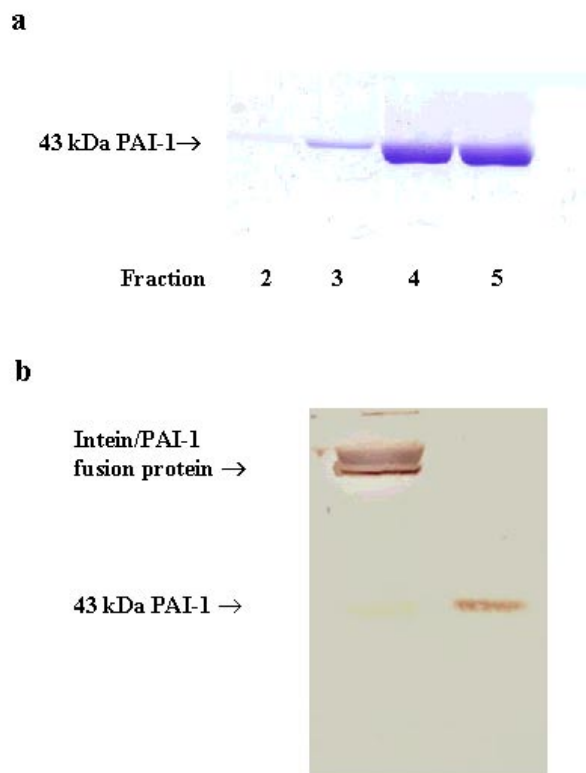


Figure 2. a: SDS-PAGE of purified 14-1b human PAI-1. Five fractions were eluted from the beads column (each 8-ml of volume), b: western blot analysis of the purified 14-1b human PAI-1.

As shown in Figure 3 f, inhibition in the number of sprout formed by aggregates was also examined. 14-1b PAI-1 at concentration: 1.0; 2.0; and 3.0 μ M showed statistically significant reduction of number sprouts formed. Synthetic inhibitors of u-PA showed also reduction of the number sprouts formed by aggregates of endothelial cells.

Interpretation of results of inhibitory activity by sprouts formation assay should taken with some precautions. First, the analysis could be performed using 2D images but not 3D images. Therefore some of the sprouts could be omitted beneath and above the plane image of the aggregate. Second, endothelial cell aggregates are made of different number of cells. Therefore it reasonable that bigger aggregates produce larger number of sprouts than smaller one. Unfortunately to this date, there is no technique, which allows produce aggregates made of exact number of cells. It is therefore conceivable that 1b-14 PAI-1 would reduce angiogenesis even in lower concentrations than reported above.

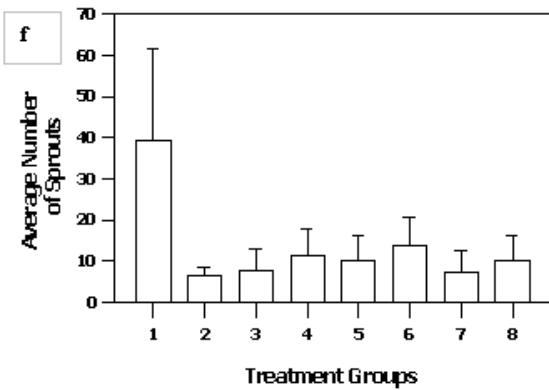
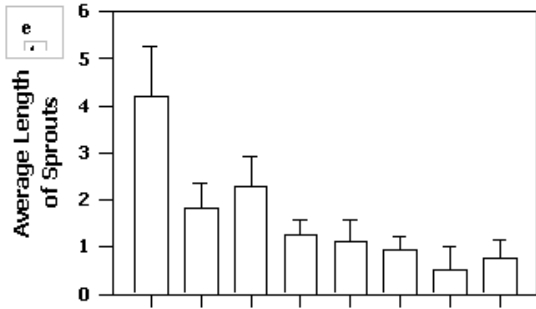
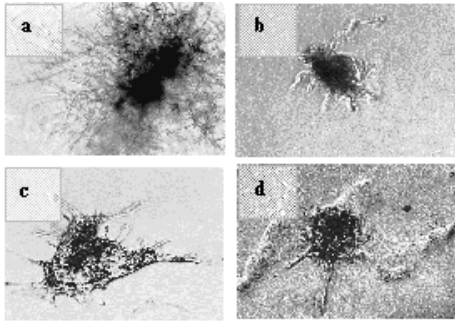


Figure 3. Inhibition of HUVEC sprout formation by recombinant 14-1b PAI-1 and synthetic inhibitors. **a**, control; **b**, 14-1b PAI-1 at concentration 5.0 μM; **c**, B-428 at concentration 12.3 μM; and **d**, benzamidine at concentration 10.6 μM. Effect of recombinant 14-1b PAI-1 in fibrin gels on the HUVEC sprout: **e**: length; and **f**: number. 1, control; 2, 0.5 μM; 3, 0.75 μM; 4, 1.0 μM; 5, 2.0 μM; 6, 3.0 μM; 7, 4.0 μM; 8, 5.0 μM.

PAI-1 14-b inhibits angiogenesis in the chicken CAM. As shown in Figure 4, 14-1b PAI-1 inhibits angiogenesis in developing chick embryos. In the control group, image analysis showed that there was essentially no difference in density of the blood vessels between the areas under the bag and areas proximal or distant to the bag. However, neovascularization was reduced under the dialysis bags containing PAI-1 in all concentration tested. With higher concentration avascular

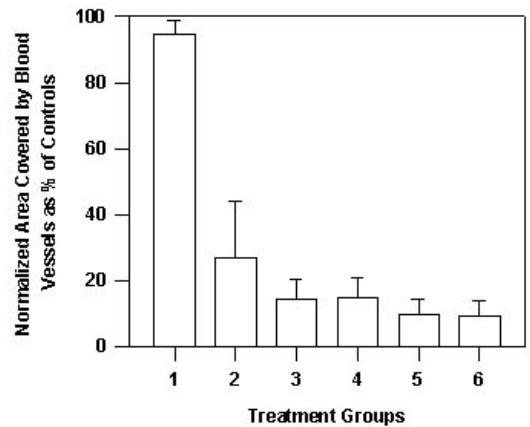
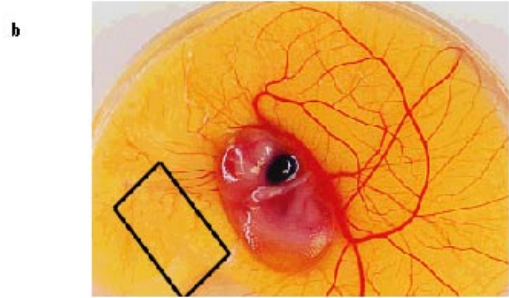
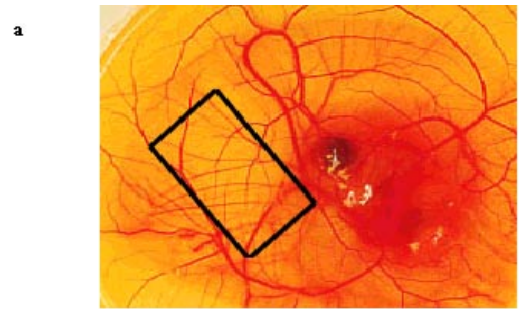


Figure 4. Photographs of 9-day old embryo **a**: control; **b**: treated by 14-1b PAI-1, 100 μM/embryo. Black rectangle indicates approximate position of dialysis bag on embryo. **c**: effect of recombinant 14-1b PAI-1 on the angiogenesis of chorioallantoic membrane 1 control group; 2, 20 μM; 3, 40 μM; 4, 60 μM; 5, 80 μM; and 6, 100 μM/embryo

zones extended beyond the edges of the bag. In addition, atrophy of existing blood vessels was observed with the application of 14-1b PAI-1. Statistical analysis revealed that the differences between the control and all five treatment groups were statistically significant and dose dependent as

it is shown in Figure 4 c. Some embryos in both control and treated groups died before the end of experiment and were not included in the results shown.

Very similar results of inhibition of angiogenesis by endogenously added PAI-1 has been reported recently (27). The authors suggest, as we do, that the inhibition of angiogenesis involves the inhibition of chicken proteinase activity by human 14-1b PAI-1. Additionally, they postulated that PAI-1 is involved independently of the protease activity pathway that includes

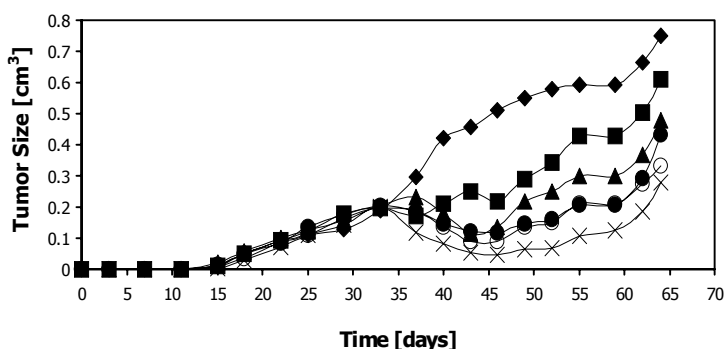


Figure 5. Tumor size of the prostate LNCaP xenografts as a function of time: ♦ Control group; ■ Saline group; ▲, 10 nM; ×, 20 nM; ○, 30 nM; ●, 40 nM. For clarity error bars are omitted. At the end of experiment tumor size was as follows: ♦, 0.75 ± 0.23 ; ■, 0.61 ± 0.09 ; ▲, 0.47 ± 0.25 ; ×, 0.27 ± 0.18 ; ○, 0.33 ± 0.13 ; ●, 0.43 ± 0.30 cm³.

binding of PAI-1 to vitronectin. The fact that the non-proteinase inhibitory PAI-1 mutants as well as antibodies against vitronectin significantly reduce angiogenesis strongly supports that the interaction with vitronectin might play important role in angiogenesis (27).

14-1b PAI-1 inhibits tumor formation in SCID mice. Thirty-two days after inoculation tumors reached an average size of 0.2 cm³ (size distribution of 0.04 - 0.41 cm³). Then animals were divided into 6 groups (n = 7) with a similar tumor size distribution. As seen in Figure 5, 14-1b PAI-1 inhibits LNCaP tumor growth in SCID/Balb-c mice. The most prominent inhibitory effect was observed at a concentration of 20 nM, at which one animal showed complete remission of the tumor. Another complete remission of tumor growth was seen in one animal at the 40 nM concentration of 14-1b PAI-1. At the beginning of 14-1b PAI-1 therapy the tumors in all treatment groups started to shrink, however with the progress of the experiment they started to grow as shown in Figure 5. Regrowth of tumors was expected, since the half-life of 14-1b PAI-1 is 156 h or 6.5 days leaving approximately 3% of the original activity in the end of experiment. Consequently as inhibitory and protective activity of PAI-1 diminishes the growth of LNCaP tumors was observed. In the control group where animals were not subjected to any surgical procedures, LNCaP tumors grew exponentially. In the Saline group where animals received 0.9% NaCl solution, rate of tumor growth was lower, and at day 40 one animal with a large tumor was euthanized. Therefore, observed differences between two control groups could be attributed to this fact.

There was statistically significant reduction in tumor size that last about 10 days post implantation of osmotic pumps at all concentration, at which time tumor re growth occurred. The strongest inhibitory effect was observed in animals treated with PAI-1 at the 20 nM concentration. Higher concentrations of PAI-1 did not produce a better effect contrary to our expectations. A similar effect was observed before with a different angiostatic agent sulindac sulfonate using a Balb/c mouse model (26). We do not have solid evidence of probable mechanism of this phenomenon. However it may be possible that PAI-1 at a higher concentration produce a thrombus envelope in the proximity of the osmotic pump effectively reducing transportation of PAI-1 into the circulation.

Reduction of angiogenesis and tumor size in animals by synthetic inhibitors of uPA has been shown by many independent studies (5-10, 17, 19, 22, 27). However, studies examining a role of PAI-1 in tumor growth and angiogenesis have been somewhat controversial. Some studies show a reduction of tumor size when animals were injected with PAI-1 or when cancer cells were transformed with PAI-1 (10, 30). Additionally, while replication-deficient adenovirus vector was used for the *in vivo* transfer of plasminogen activator inhibitor type 1 (PAI-1) cDNA resulted in a 50% reduction in the number of animals developing liver metastases; and a 78% reduction in the metastatic tumor burden in animals that eventually developed metastases. Conversely, two other studies using PAI-1 deficient mice showed no effect on tumor growth (29) or that tumor angiogenesis requires PAI-1 (28). These somehow conflicting results could be attributed to the amount of PAI-1 produced by different transgenic animals or the short half-life of PAI-1 used in these experiments. In all these studies wild type PAI-1 was used. However, when PAI-1 with an extended half-life was used, dramatic inhibitory effects were observed. Impressive inhibition of angiogenesis by 14-1b PAI-1 has been shown in Stefansson paper (27) as well as dramatic reduction of angiogenesis and tumor size presented in this paper strongly support this hypothesis. It is also possible, as Stefansson proposed that PAI-1 in association with vitronectin could regulate angiogenesis in separate but likely overlapping pathways. First, by inhibiting proteinase activity, and second by binding to vitronectin. In this model vitronectin might promote vascular cell migration and PAI-1 by controlling access to the vitronectin would regulate the enhancement of angiogenesis (27). It is therefore plausible that wild type PAI-1 binds to vitronectin and stimulates angiogenesis in low concentrations while higher amounts or longer half-live PAI-1 can suppress the stimulation of angiogenesis by inhibiting proteolytic pathway.

In conclusion, regardless of the mechanism of action, the present study demonstrates that exogenously applied 14-1b PAI-1 is a powerful inhibitor of angiogenesis and a powerful anti-cancer agent.

Acknowledgments

This work was supported in part by grants from: American Diagnostica Inc., Greenwich, CT., and Ohio Board of Regents. The uPA was generous gift from Dr. R. Hart (American Diagnostica Inc., Greenwich, CT), PAI-1 clone 14-1b was generous gift from Dr. D. Ginsburg (University of Michigan, Ann Arbor, MI). We would like to thank Dr. Yasser Saad from the Cleveland Clinic Foundation, Cleveland, OH and Mr. Duane Day

from Molecular Innovation, Inc., Royal Oak, MI for critical suggestions and discussions.

Reference

- Conese M, Blasi F: The urokinase/urokinase-receptor system and cancer invasion. *Clinical Hematology* 8(2): 365-389, 1995.
- Festuccia C, Vincentini C, di Pasquale AB. *et al*: Plasminogen activator activities in short-term tissue cultures of benign prostatic hyperplasia and prostatic carcinoma. *Oncology Research* 7(3-4): 131-138, 1995.
- Achbarou A, Kaiser S, Tremblay G, *et al*: Urokinase overproduction results in increased skeletal metastasis by prostate cancer cells in vivo. *Cancer Research*, 54(9): 2372-2377, 1994.
- Wilson MJ, Sinha AA: Plasminogen activator and metalloproteinase activities of DU-145, PC-3, and 1-LN-PC-3-1A human prostate tumors grown in nude mice: Correlation with tumor invasion behavior. *Cellular and Molecular Biology Research*, 39(8): 751-760, 1993.
- Ossowski L: In vitro invasion of modified chorioallantoic membrane by tumor cells: The role of cell surface-bound urokinase. *Journal of Cell Biology*, 107: 2437-2445, 1988.
- Billstrom A, Hartley-Asp B, Lancander I. *et al*: The Urokinase inhibitor p-aminobenzamidine inhibits growth of a human prostate tumor in SCID mice. *International Journal of Cancer*, 61(4): 542-547, 1995.
- Sparks RL, Pool TB, Smith NK, Cameron IL: Effects of amiloride on growth and intracellular element content of tumor cells in vivo. *Cancer Research*, 43(1): 73-77, 1983.
- Iishi H, Tatsuta M, Baba M, *et al*: Suppression by amiloride of bombesin-enhanced peritoneal metastasis of intestinal adenocarcinomas induced by azoxymethane. *International Journal of Cancer* 63(5): 716-719, 1995.
- Koo JY, Parekh D, Townsend CM. Jr, *et al*: Amiloride inhibits the growth of human colon cancer cells in vitro. *Surgical Oncology* 1(6): 385-389, 1992
- Jankun J, Keck RW, Selman SH, Skrzypczak-Jankun E, Swiercz R: Inhibitors of urokinase restrict growth of prostate cancer xenografts in severe combined immunodeficient mice. *Cancer Research* 57: 559-563, 1997.
- Jankun J, Merrick WH, Goldblatt PJ: Expression and localization of elements of the plasminogen activation system in benign breast disease and breast cancers. *Journal of Cellular Biochemistry* 53(2): 135-144, 1993.
- Jankun J, Maher VM, McCormick JJ: Malignant transformation of human fibroblasts correlates with increased activity of receptor bound plasminogen activator. *Cancer Research* 51(4): 1221-1226, 1991
- Kwaan HC, Keer HN, Radosevich JA, *et al*: Components of the plasminogen-plasmin system in human tumor cells. *Seminars in Thrombosis and Hemostasis* 17: 175-182, 1991.
- Tucker HM, Mottonen J, Goldsmith EJ, Gerard RD: Engineering of plasminogen activator inhibitor - 1 to reduce the rate of latency. *Nat Struc Biol* 2: 442-445, 1995.
- Mottonen J, Strand A, Symersky J, *et al*: Structural basis of latency in plasminogen activator inhibitor-1. *Nature* 355: 270-273, 1992.
- Sharp AM, Stein PE, Pannu NS, *et al*: The active conformation of plasminogen activator inhibitor 1, a target for drugs to control fibrinolysis and cell adhesion. *Structure Fold Des* 15,7(2):111-118, 1999.
- Hasuda K, Lee C, Tannock IF: Antitumor Activity of Nigericin and 5-(N-ethyl-N-isopropyl) amiloride: an approach to therapy based on cellular acidification and the inhibition of regulation of intracellular pH. *Oncology Research* 6(6): 259-268, 1994.
- Pepper MS: Upregulation of urokinase receptor expression on migrating endothelial cells. *J Cell Biol* 122: 673-676, 1993
- Swiercz R, Skrzypczak-Jankun E, Merrell MM, *et al*: Angiostatic Activity of Synthetic Inhibitors of Urokinase Type Plasminogen Activator. *Oncology Reports* 6: 523-526, 1999.
- Jankun J, Skrzypczak-Jankun E: Molecular Basis of Specific Inhibition of Urokinase Plasminogen Activator by Amiloride. *Cancer Biochemistry Biophysics* 17: 1-2, 109-123, 1999.
- Goodson RJ, Doyle MV, Kaufman SE, *et al*: High-affinity urokinase receptor antagonists identified with bacteriophage peptide display. *Proc Natl Acad Sci U S A* 19;91(15):7129-7133, 1994.
- Ignjatovic Z, Nikolic L: Inhibition of angiogenesis in the cornea with amiloride. *Srp Arh Celok Lek* 124(5-6):120-3, 1996.
- Pepper MS, Vassalli JD, Montesano R, *et al*: Urokinase-type plasminogen activator is induced in migrating capillary endothelial cells. *J Cell Biol* 105: 2535-2541, 1985.
- Lawrence DA, Berkenpas MB, Palaniappan S, *et al*: Localization of vitronectin binding domain in plasminogen activator inhibitor-1. *J Biol Chem* 27;269(21):15223-15228, 1994.
- Lawrence DA, Olson ST, Palaniappan S, *et al*: Engineering plasminogen activator inhibitor 1 mutants with increased functional stability. *Biochemistry* 33:12: 3643-3648, 1994.
- Skopinska-Rozewska E, Skurzak H, Bialas-Chromiec B, *et al*: The effect of various synthetic and natural substances on tumor growth and angiogenesis. *International Journal of Molecular Medicine* 6:(S1), 52, 2000.
- Stefansson S, Petitclerc E, Wong MK, *et al*: Inhibition of Angiogenesis in vivo by Plasminogen Activator Inhibitor-1. *J Biol Chem* 2000 Nov 16; [e-pub ahead of print]
- Bajou K, Noel A, Gerard RD, *et al*: Absence of host plasminogen activator inhibitor 1 prevents cancer invasion and vascularization. *J M Nat Med* 4(8): 923-8, 1998.
- Eitzman DT, Krauss JC, Shen T, *et al*: Lack of plasminogen activator inhibitor-1 effect in a transgenic mouse model of metastatic melanoma. *Blood* 1;87(11):4718-22, 1996.
- Soff GA, Sanderowitz J, Gately S, *et al*: Expression of plasminogen activator inhibitor type 1 by human prostate

- carcinoma cells inhibits primary tumor growth, tumor-associated angiogenesis, and metastasis to lung and liver in an athymic mouse model. *J Clin Invest* 96(6): 2593-600, 1995.
31. Hollas W, Hoosein N, Chung LW, *et al*: Expression of urokinase and its receptor in invasive and non-invasive prostate cancer cell lines. *Thromb Haemost* 7;68(6): 662-6, 1992.
 32. InsightII, 95.0/3.0.0. User Guide
 33. Flores TP, Orengo CA, Moss DS, *et al*: Comparison of conformational characteristics in structurally similar protein pairs. *Protein Science* 2: 1811-1826, 1993.
 34. Bordo D, Argos P: Evolution of protein cores. Constraints in point mutations as observed in globin tertiary structures. *J Mol Biol* 211: 975-988, 1990.
 35. Sanger F: Determination of nucleotide sequences in DNA. *Science* 11;214(4526):1205-1210, 1981.